

Battery Grading Algorithm in 2nd-Life Repurposing Li-ion Battery System

Ya Lv, Benjamin Ong Wei Lin, Wanli Niu, Benjamin Seah Chin Tat

Abstract—This article presents a methodology that improves reliability and cyclability of 2nd-life Li-ion battery system repurposed as energy storage system (ESS). Most of the 2nd-life retired battery systems in market have module/pack-level state of health (SOH) indicator, which is utilized for guiding appropriate depth of discharge (DOD) in the application of ESS. Due to the lack of cell-level SOH indication, the different degrading behaviors among various cells cannot be identified upon reaching retired status; in the end, considering end of life (EOL) loss and pack-level DOD, the repurposed ESS has to be oversized by > 1.5 times to complement the application requirement of reliability and cyclability. This proposed battery grading algorithm, using non-invasive methodology, is able to detect outlier cells based on historical voltage data and calculate cell-level historical maximum temperature data using semi-analytic methodology. In this way, the individual battery cell in the 2nd-life battery system can be graded in terms of SOH on basis of the historical voltage fluctuation and estimated historical maximum temperature variation. These grades will have corresponding DOD grades in the application of the repurposed ESS to enhance the system reliability and cyclability. In all, this introduced battery grading algorithm is non-invasive, compatible with all kinds of retired Li-ion battery systems which lack of cell-level SOH indication, as well as potentially being embedded into battery management software for preventive maintenance and real-time cyclability optimization.

Keywords—Battery grading algorithm, 2nd-life repurposing battery system, semi-analytic methodology, reliability and cyclability.

I. INTRODUCTION

LI-ION Batteries, as high energy density and cost effective solution, are deriving more and more system solutions in applications of electric mobility, stationary and maritime. After being first commercialized in 1991, Li-ion batteries are now growing at double digit rates [1] and its market share is expected to double in the next five years. Demand for Li-ion batteries in electric mobility is forecasted to increase over 16 times to 2333 gigawatt hours in 2030 [2]. This much growth is not all good however, as the number of batteries explodes from demand, a serious challenge for waste-management appears. Worldwide, it is expected to produce over 2 million metric tons of used batteries per year by 2030 [3]. There is now an e-waste “timebomb” of sorts, to which, a solution must be found accordingly. Waste management practices such as battery recycling are already being used today, however it is not a cheap process. Lithium obtained through mining is about five times cheaper than lithium obtained through recycling. This has led researchers and manufacturers to explore ‘2nd-life’ battery reprocessing. This concept simply refers to reusing any

batteries that do not met the criteria for application in automotive vehicles instead of disposing of the battery. Batteries retired from automotive use retain about 70-80% of their original capacity and thus, are still fit for less demanding applications such as a stationary ESS [16]. The usage of 2nd-life batteries over newly manufactured ones drastically reduces the upfront cost due to batteries often making up the largest portion of the total cost. One of the challenges faced is the lack of post-life evaluation of battery health; thus, in this paper, we propose a robust SOH grading algorithm for repurposing 2nd-life battery system with better reliability and cyclability.

II. TRADITIONAL SOH ALGORITHMS

State of Health

SOH represents the difference of the battery state between the life beginning and end, in percentage. A battery will reach its EOL when the battery cannot meet the minimum requirements as defined. The capacity fading is defined when the battery capacity dropped to about 70-80% of the rated value. The power fading is defined when the maximum power dropped to about 70-80% of the rated value. Overall, SOH describes the severity of battery degradation [4].

Battery aging will induce performance changes. In both e-mobility and stationary applications, battery internal resistance and capacity will degrade when a battery ages. Therefore, the changes in internal resistance or that in capacity, can be used to measure battery SOH [4]. In past years, various approaches have been proposed to estimate SOH of Li-ion battery, which can be summarized as three types: mode-free, model-based and artificial intelligence based. The model-free approach defines battery SOH as $SOH = \frac{C_{aged}}{C_n} * 100\%$, $SOH = \frac{R_{aged}}{R_n} * 100\%$ where C_{aged} and R_{aged} indicate aged capacity and internal resistance, and C_n and R_n represent nominal capacity and internal resistance of new battery. Model-based approach has enclosed battery equivalent circuit model (ECM) [5] and electrochemical model [6], in which different observers are utilized to estimate operational capacity and internal resistance, such as particle filters [7] and Kalman filters [8]. Artificial intelligence approach has an applied machine learning/deep learning algorithm to estimate battery SOH, such as clustering, neural network [9].

The key stress factors associated with battery aging are temperature, state of charge (SOC) and current. Their respective influence is elaborated as below:

Ya Lv is with Durapower Technology, Singapore (e-mail: laylaneylv@gmail.com).

A. Temperature

Li-ion battery has optimal operating temperature 15 °C to 35 °C to guarantee its working reliability and maintain its maximum cyclability [10]. Temperature effect exists in both calendar aging and cycling aging modes.

At high temperature [11], the solid-electrolyte-interfacial (SEI) layer will deteriorate slowly and gradually dissolve into the electrolyte, the damaged SEI layer will be restored from the side reactions between the exposed active anode material and electrolyte. In this restored SEI layer, some metastable organic SEI components are converted into stable inorganic molecules because of the higher temperatures, which are more stable and less porous. Parts of the cathode will dissolve into the electrolyte and become part of the SEI layer as well. As a result, the intercalation at the anode will be more difficult and ionic conductivity will be lowered. The same degradation mechanism occurs at the cathode side with solid-permeable-interface (SPI) layer, causing structural damage to the active cathode material. At above 70 °C the threat of thermal runaway appears [12]. At low temperature, there is sluggish electrochemical reaction [13], which will induce output power degrading and irreversible capacity loss.

The relationship between the capacity fading and temperature is represented in Arrhenius equation [11], $A = A_0 \cdot \exp\left(-\frac{E_a}{RT}\right)$ where A is the amount of capacity fading, A_0 is the pre-exponential term, E_a is the activation energy, R is the gas constant and T is the temperature in Kelvin. This equation is applicable to describe both calendar fade and cycling fade. The activation energy E_a decreases at higher battery SOC, which means that capacity fades faster at higher battery SOC.

B. State of Charge

SOC represents the available capacity in the battery, in percentage. At high SOC [11], more electro-chemical reactions will take place and the SEI layer will grow faster, as well as the aggravating self-discharge. At the same time, the occurred electrolyte oxidation will increase battery impedance, which results in capacity fading. In cycling mode, the SOC effect on battery degradation cannot be described well owing to short maintain time at different SOC. Usually, a boundary for high SOC and low SOC will be suggested, namely the advised DOD, in the battery system.

C. Current

Current inevitably impacts on battery fading due to the generated ohmic heat power. The generated ohmic heat power can be described as $P_{ohm} = I_i^2 R_i$ where I_i is the current flowing through battery internal resistance and R_i the battery internal resistance. High current affects battery aging in the similar way as high temperature caused by the uprising ohmic heat power.

Apart from ohmic heat influence, high continuous current can cause overpotential of electrodes due to inefficient diffusion rate of lithium ions. In addition to the overpotential effect, high continuous current aggravates deformation and loss of active materials by bringing extra strain on electrodes. Overall, high continuous current has to be avoided to prolong battery life.

III. PROBLEMS WITH TRADITIONAL SOH ALGORITHMS IN THE APPLICATION OF 2ND-LIFE BATTERIES

Today, most of the retiring battery packs have battery management systems (BMS) that use the variables described above in order to calculate SOH on a module/pack-level. Newly manufactured batteries have quality control and manufacturing tolerances that ensure all batteries produced will perform to the same or close standard. Thus, batteries are considered similar and the sensors that would gather information on these variables are commonly designed to gather module/pack-level data. While this management strategy is viable for new batteries or batteries operating during their intended lifespan, batteries operating pass their intended lifespan will not be managed well using the same strategy. Especially when the 2nd-life e-mobility battery system is repurposed as a stationary ESS, the different application conditions will require an adjustable managing strategy.

Because the BMS calculates SOH for the entire module/pack, the degradation status distribution in the cells of module/pack cannot be reflected in existing management strategy. Given that the BMS algorithm cannot identify the healthier cells with less degradation and unhealthier cells with more degradation, the inefficiencies will occur where healthier cells with less degradation will not be used to their full potential and unhealthier cells with more degradation than the others will be charged and discharged beyond their safe region, which may cause catastrophic damage. Although this issue has mostly been solved in newer battery module/pack models with updated BMS algorithms and internet of things (IoT) sensors accumulating cell-level signal in real-time way, little has yet been done about the existing generation of battery systems that are retiring which do not have these advanced algorithms. The massive changes required in hardware and software are becoming big challenges when solving degradation status distribution in 2nd-life battery systems. This article aims to address this issue with non-invasive battery grading algorithm by making use of historical data and our developed semi-analytic methodology [14].

IV. NON-INVASIVE BATTERY GRADING ALGORITHM

The non-invasive battery grading algorithm flowchart can be found in Fig. 1.

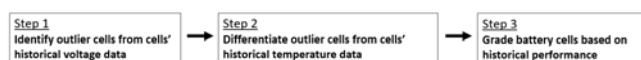


Fig. 1 Non-invasive battery grading algorithm flowchart

A. Identifying Outlier Cells from Historical Voltage Data

We have chosen Durapower [15] e-bus battery system as study example, as indicated in Fig. 2. Part of historical voltage data in the battery system is shown in Fig. 3, from which the charging and discharging voltage variation can be seen. There is similarity and difference among the 27 cells in terms of voltage variation.

As learned in engineering experience, the deeper degraded battery cell usually generates bigger ripple in its voltage curve. Therefore, we come up below sorting procedures to identify the outlier cells in terms of voltage impact on battery degradation.

- Procedure 1: For every cell, a maximum voltage fluctuation in reference to its mean value along with time is calculated as ΔV_{m-i} , as shown in Fig. 4.
- Procedure 2: Averaging ΔV_{m-i} among 27 cells to be ΔV^* .
- Procedure 3: Calculating the ratio between ΔV_{m-i} and ΔV^* to separate cells with ratio bigger than 1 from the cells with ratio smaller than 1, as seen in Fig. 5.

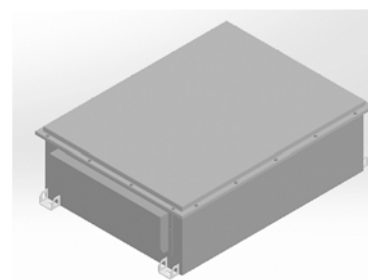


Fig. 2 Durapower Li-ion battery system

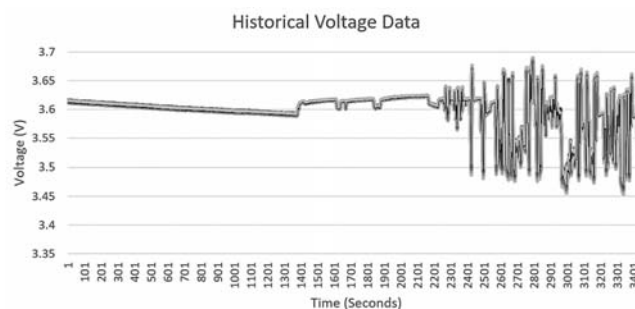


Fig. 3 Historical voltage data in Durapower battery system

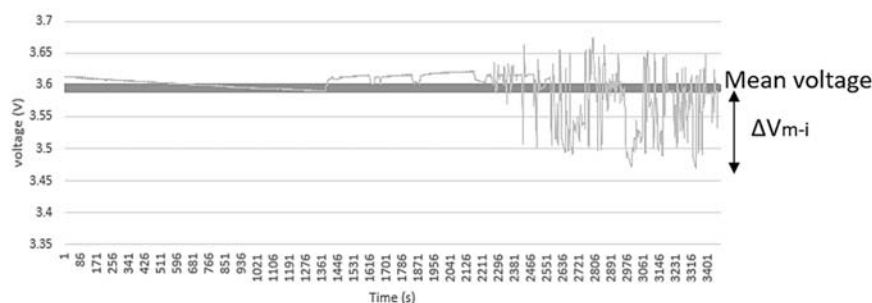


Fig. 4 Cell voltage maximum fluctuation

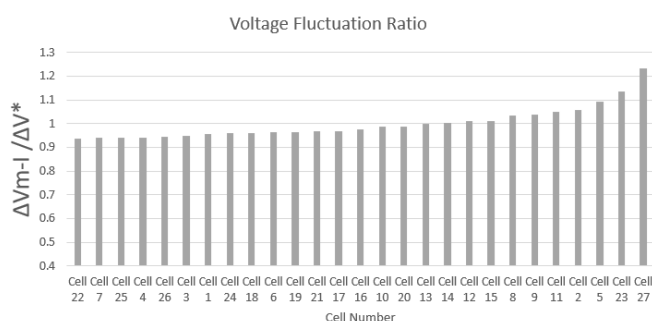


Fig. 5 Calculation to categorize cells in terms of voltage max fluctuation amplitude

B. Differentiating Outlier Cells from Historical Temperature Data

A historical heavy-loading current data of the 27 cells were assumed in this article, as displayed in Fig. 6. By adopting the cell properties of Durapower battery system, we can estimate the historical heat power curve on basis of the current data and assumed system-level SOH, as shown in Fig. 7. In this battery system, Nickel-Manganese-Cobalt Oxide (NMC) 30Ah Li-ion pouch cells manufactured in Durapower are used in the system,

system SOH of 0.8 is assumed in calculation of heat power.

According to our developed Semi-Analytic Methodology (SAM) [14], a simulation reference case of the studied battery system is needed to compose the SAM model, as illustrated in Fig. 9. In this article, 27 SAM models have been generated to evaluate thermal performance of the 27 cells effectively. Based on the thermal simulated reference case in Fig. 8 and 27 SAM models, the historical temperature curves of the 27 cells can be calculated, as shown in Fig. 10.

It can be found in Fig. 10 that the battery cell maximum temperature reached above 40 °C in the heavy-loading history. The optimal working temperature range 15 °C to 35 °C [10] of Li-ion battery cells and temperature influence on battery cell degradation have been explained before, once cell temperature is above 35 °C, the higher the temperature, the more capacity fading generated, as explained in Arrhenius equation [11]. Therefore, we refer below to the procedures to differentiate the outlier cells in terms of temperature impact on battery degradation.

- Procedure 1: For every cell, the biggest deviation of historical maximum temperature from 35 °C is calculated as ΔT_{m-i} , as shown in Fig. 11.

- Procedure 2: Averaging ΔT_{m-i} among 27 cells to be ΔT^* .
- Procedure 3: Calculating the ratio between ΔT_{m-i} and ΔT^* to separate cells with ratio bigger than 1 from the cells with ratio smaller than 1, as seen in Fig. 12.

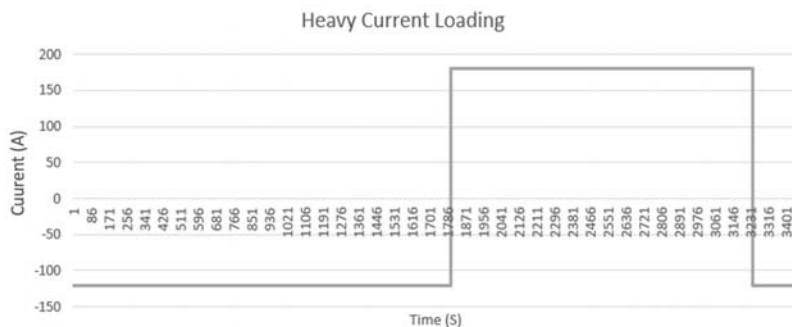


Fig. 6 Assumed heavy-loading current data

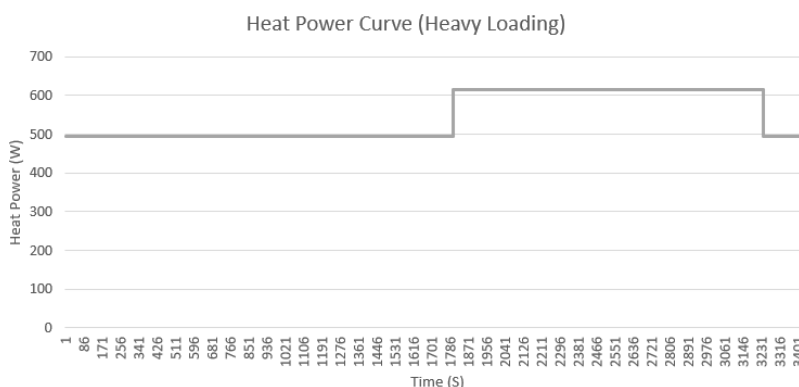


Fig. 7 Heat power generated based on assumed current curve

| $T_{fluid}^{inlet}, ^\circ C$ | $m_{fluid}, kg/s$ | q_{tot}, W | $C_{fluid}, J/kg/K$ | T_s, s | $T_{cell}^0, ^\circ C$ | m_{cell}, kg | $C_{th,i}, J/kg/K$ | $T_{hottest\ cell}, ^\circ C$ | $T_{outlet\ fluid}, ^\circ C$ |
|---------------------------------|-------------------|------------------|------------------------|----------|--------------------------------------|-----------------------|-----------------------|---------------------------------|----------------------------------|
| 20 | 0.0057 | 100 | 1006.51 | 1800 | 20 | 111.52 | 678 | 21.99 | 20.8 |
| Fluid inlet average temperature | Mass flowrate | Total heat power | Heat capacity of Fluid | Time | Initial temperature of battery cells | Mass of battery cells | Heat capacity of cell | Max temperature of hottest cell | Fluid outlet average temperature |

Fig. 8 Thermal Simulation Reference Case results

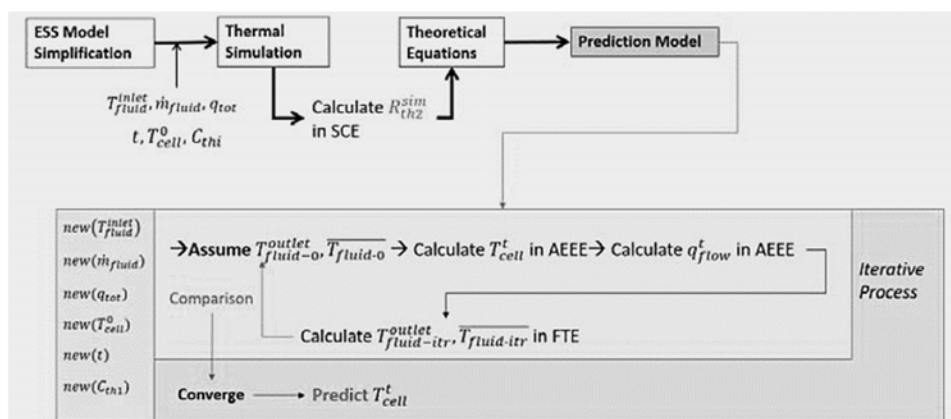


Fig. 9 SAM architecture procedures in transient analysis [14]

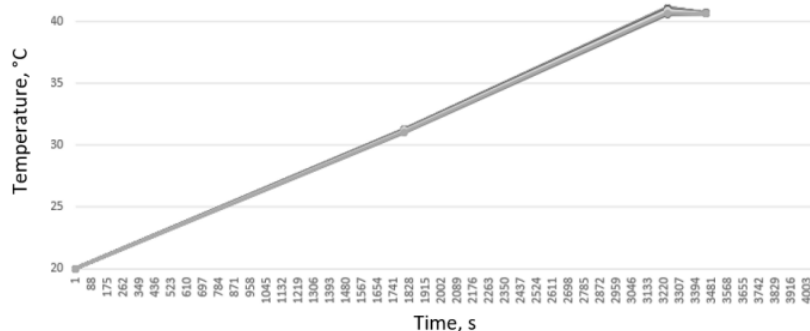


Fig. 10 Calculated historical temperature curves based on SAM [14] methodology

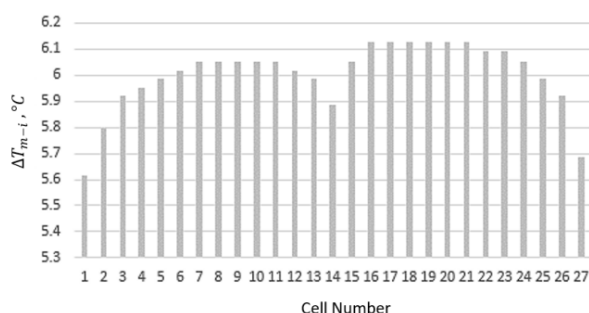


Fig. 11 Historical maximum temperature deviation distribution among 27 cells

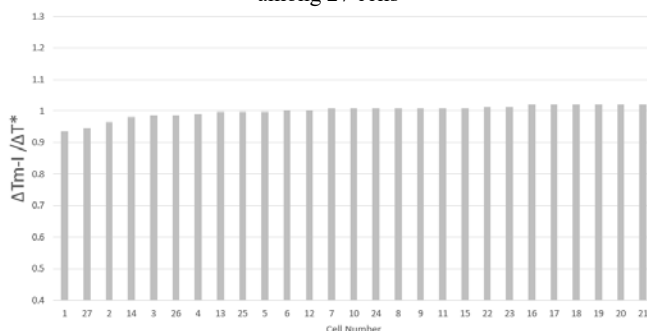


Fig. 12 Calculation to categorize cells in terms of maximum temperature deviation from optimal bar

C. Grade Battery Cells

In Subsections A and B, we categorize battery cells respectively from perspective of historical cell voltage max fluctuation amplitude and historical cell maximum temperature deviation from optimal bar. By consolidating analysis results from Subsections A and B, we grade battery cells obeying rules shown in Fig. 13. Correspondingly, the grading results of 27 battery cells can be found in Figs. 14 and Fig. 15.

As shown in Fig. 15, we can see that the grade A cells are cell no. 1, 3, 4, 13, 25, 26; grade C cells are cell no. 8, 9, 11, 12, 15, 23; the others belong to grade B. This result can guide engineers to set different DOD grades when repurpose the 2nd-life battery system as a stationary ESS; in this way, the reliability and cyclability can be greatly optimized and improved.

| Grades | $\Delta V_{m-i} / \Delta V^*$ | $\Delta T_{m-i} / \Delta T^*$ |
|---------|-------------------------------|-------------------------------|
| Grade A | <1 | <1 |
| Grade B | <=1 | >=1 |
| | >=1 | <1 |
| Grade C | >1 | >1 |

Fig. 13 Grading rules in light of voltage and temperature historical performance of battery cells

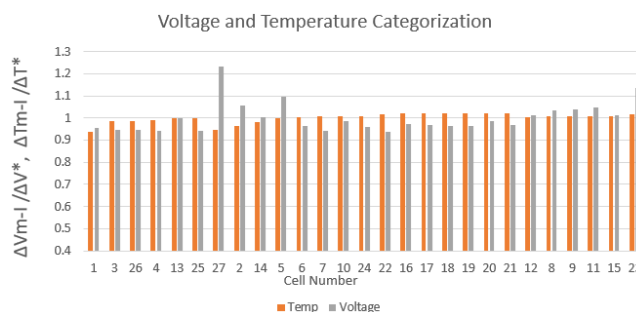


Fig. 14 Display of voltage fluctuation amplitude and temperature deviation from optimal bar of 27 cells

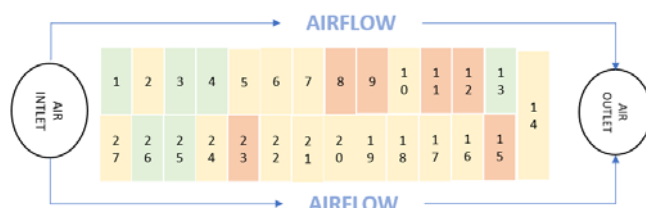


Fig. 15 Grading results of 27 cells in system planar diagram, in which green indicates grade A, yellow indicates grade B, red indicates grade C

V. RESULTS ANALYSIS

A. Results So Far

As illustrated in this article, the key stress factors to influence battery aging are temperature, current and SOC. In this proposed battery grading algorithm, on one hand, cell-level historical voltage data as a reflection of cell degradation are

investigated, while on the other hand, cell-level historical maximum temperature data, which are calculated using our developed SAM methodology [14], are also investigated for their effect on degradation. Although there is lack of cell-level SOC data, the SOC influence in cycling fade mode is unstable originally. In all, the proposed battery grading algorithm can realize and identify degradation distribution among cells in battery system, even though there are three grades only.

B. Future Research

As to next steps, the historical storage data are expected to be reviewed, in order to take into account calendar degradation mode. At the same time, while the 2nd-life battery cells in the system are well graded in terms of SOH, the corresponding DOD grading will be necessary to better apply them. A series of testing and further research will be indispensable to explore the correlation between battery degradation grades and DOD grades, which would combine to achieve the promised improvement in terms of reliability and cyclability.

C. Conclusion

In conclusion, this article presents a battery grading algorithm which is non-invasive and designed for repurposing 2nd-life Li-ion battery system. Before we can reap the benefits of 2nd-life battery systems we must solve the issue of having effective post-life battery cell SOH evaluation first. Furthermore, the battery degradation grading will be correlated with the DOD grading in the future, thus achieving massive improvement in terms of reliability and cyclability. Although these changes would raise up big challenges to BMS and power conditioning systems, it would also open many opportunities to revolutionize the whole life cycle of Li-ion batteries from its 1st-lifetime use to 2nd-lifetime use until its disposal.

REFERENCES

- [1] <https://www.prnewswire.com/news-releases/second-life-automotive-lithium-ion-battery-market-to-grow-with-massive-cagr-through-2030-ps-intelligence-301174300.html>
- [2] <https://www.statista.com/statistics/1103401/predicted-lithium-ion-battery-capacity-by-company/>
- [3] <https://cen.acs.org/materials/energy-storage/time-serious-recycling-lithium/97/i28>
- [4] Kailong LIU, Kang LI, Qiao PENG, Cheng ZHANG, A brief review on key technologies in the battery management system of electric vehicles
- [5] Nejad S, Gladwin D T, Stone D A. A systematic review of lumped parameter equivalent circuit models for real-time estimation of lithium-ion battery states. *Journal of Power Sources*, 2016, 316: 183–196
- [6] Berecibar M, Gandiaga I, Villarreal I, et al. Critical review of state of health estimation methods of Li-ion batteries for real applications. *Renewable & Sustainable Energy Reviews*, 2016, 56: 572–587
- [7] Bi J, Zhang T, Yu H, et al. State-of-health estimation of lithium-ion battery packs in electric vehicles based on genetic resampling particle filter. *Applied Energy*, 2016, 182: 558–568
- [8] Gholizadeh M, Salmasi F R. Estimation of state of charge, unknown nonlinearities, and state of health of a lithium-ion battery based on a comprehensive unobservable model. *IEEE Transactions on Industrial Electronics*, 2014, 61(3): 1335–1344
- [9] You G, Park S, Oh D. Real-time state-of-health estimation for electric vehicle batteries: A data-driven approach. *Applied Energy*, 2016, 176: 92–103
- [10] Ahmad P., Shriram S. and Gi-Heon K. (2013). Large Format Li-Ion Batteries for Vehicle. Available: Applications (<http://www.nrel.gov/docs/fy13osti/58145.pdf>)
- [11] Long Lam, University of Technology Delft, 23 August 2011. A Practical

Circuit based Model for State of Health Estimation of Li-ion Battery Cells in Electric Vehicles

- [12] Woodbank Communications Ltd (2005). Battery and Energy Technologies: Lithium Battery Failures. Available: http://www.mpoweruk.com/lithium_failures.htm
- [13] Agwu Daberechi D., Opara F. K., Chukwuchekwa N, Dike. D. O., Uzoechi L., Department of Electrical and Electronic Engineering, Federal University of Technology, Owerri. (FUTO), Nigeria. Review of Comparative Battery Energy Storage Systems (Bess) for Energy Storage Applications in Tropical Environments
- [14] Ya Lv. Semi-Analytic Method in Fast Evaluation of Thermal Management Solution in Energy Storage System
- [15] <https://www.durapowerbattery.com/>
- [16] Lluc Canals CasalsB. Amante GarcíaCamille Cana. Second life batteries lifespan: Rest of useful life and environmental analysis